

# Aluminum-Silicon Carbide Coatings by Plasma Spraying

K. Ghosh, T. Troczynski, and A.C.D. Chaklader

(Submitted 26 Dec 1996; in revised form 14 Oct 1997)

**An aluminum base composite (Al-SiC) powder has been developed for producing plasma sprayed coatings on Al and other metallic substrates. The composite powders were prepared by mechanical alloying of 6061 Al alloy with SiC particles. The concentration of SiC was varied between 20 and 75 vol%, and the size of the reinforcement was varied from 8 to 37  $\mu\text{m}$  in the Al-50 vol%SiC composites. The 44 to 140  $\mu\text{m}$  composite powders were sprayed using an axial feed plasma torch. Adhesion strength of the coatings to their substrates were found to decrease with increasing SiC content and with decreasing SiC particle sizes. The increase in the SiC content and decrease in particle size improved the erosive wear resistance of the coatings. The abrasive wear resistance was found to improve with the increase in SiC particle size and with the SiC content in the composite coatings.**

**Keywords** abrasion and erosion resistance, mechanical alloying, metal matrix composites (MMC), peel adhesion strength, process control additives (PCA)

## 1. Introduction

The issues of global warming and carbon dioxide emission levels are forcing automobile manufacturers to reduce the consumption of fossil fuels and increase energy efficiency. Reduction in the weight of the automobiles is one of the better alternatives. The cylinder block is one of the main components of the engine blocks that dominates its overall weight. Thus, reduction in the weight of the cylinder block by replacing the cast iron ( $\rho = 7.5 \text{ g/cm}^3$ ) with Al ( $\rho = 2.7 \text{ g/cm}^3$ ) offers a reduction in the overall weight. Hence, a substantial amount of research is directed toward manufacturing the cylinder blocks with Al and its alloys (Ref 1, 2).

The use of Al as a cylinder block is limited by the poor abrasion and wear resistance of Al; this is critical for the cylinder bores. Research efforts are being directed to produce Al cylinder blocks with cast (gray) iron liners (Ref 1). To improve the compatibility and remove the inherent differences between the cast iron liners and the Al cylinder blocks, Al base metal matrix composites (MMC) which have abrasion and wear resistance properties equal to or better than cast iron are an attractive solution.

The specialized technology required in the casting of a cylinder block does not permit the manufacture of a monolithic MMC structure, and hence, coatings or MMC liners in the cylinder bores of Al engines are preferred. At present, these wear resistant surfaces are formed mainly by casting or preform routes (Ref 1, 2). The high cost of the casting technologies, such as squeeze casting and die casting, and the subsequent machining of the liners limit the process to high priced cars (Ref 2).

The choice of the coating material for a monolithic Al component depends on weight savings, heat transfer, compatibility, and performance factors (Ref 3, 4). Thus, although different metal matrix composites show better wear resistance than cast iron, Al-SiC composite coatings are gaining popularity for these types of applications. The composites, having a density range of 2.7 to 3.2  $\text{g/cm}^3$  depending on the SiC content, show heat transfer, ductility, and other properties similar to the Al substrate.

One important factor in obtaining a good plasma sprayed coating is the quality of the powder which is being used for spraying (Ref 5). The uniformity of SiC in the matrix of the Al-SiC powder determines the spatial distribution of the reinforcement in the coatings. The shape and size of the particles determines the ability of the powder to flow. Compared to the commonly used processes for producing plasma sprayable composite powders—mechanical blending, fusing and crushing, agglomeration, and sintering—mechanical alloying (MA) has a few distinct advantages in producing Al-SiC composite powders (Ref 5-7). Mechanical alloying is a high energy, dry milling technique which can produce composite metal powders with a uniform distribution of the reinforcing second phase particles (Ref 8-11). Since the entire process takes place in the solid state, it can produce alloys that are otherwise impossible to produce by the conventional melting and casting or sintering techniques (Ref 12). Thus, one of the most economical processes to obtain uniformly distributed reinforcements, greater than 30 vol%, is through MA. The reinforcements can be of particulate type or whiskers, and fibers and their sizes may vary from 5 to 100  $\mu\text{m}$  (Ref 8, 9, 12-14).

There are relatively few literature reports on thermal spraying of aluminum-base composites. Ilyuschenko et al. (Ref 15) reported deposition of Al base MMC, where the reinforcing phase was SiC or TiC particles. The reinforcement varied from 50 to 75 vol%. Khor et al. (Ref 16) studied plasma sprayed Al-Li (2.54 wt%) base MMC. The reinforcement particles were electronic grade (submicron) sized SiC particles. The clustering of the SiC particles was avoided by extensive processing of the powders including fluidized bed mixing, spray drying, and milling.

K. Ghosh, T. Troczynski, and A.C.D. Chaklader, University of British Columbia, Vancouver, V6T 1Z4, BC, Canada.

The present work involved the synthesis of the MMC powders with Al as the matrix and different size SiC reinforcements. The coatings produced from the composite powders were studied for their microstructural uniformity, density, adhesion, hardness, abrasion, erosion resistance, and other physical and chemical properties. An attempt was made to optimize the wear, adhesion, and hardness of the coating, based on the SiC content and particle size.

## 2. Experimental Procedures

### 2.1 Powder Preparation

Spray dried and atomized aluminum alloy 6061 powder (Valimet Inc., Stockton, CA) of average particle size 45  $\mu\text{m}$  was mechanically alloyed with SiC particles (Norton Company, Saint Gobain, Boston, MA) of mean size 8  $\mu\text{m}$  (93% of the particles from 6 to 10  $\mu\text{m}$ ), mean size 15  $\mu\text{m}$  (94% of the particles from 12 to 18  $\mu\text{m}$ ), mean size 22  $\mu\text{m}$  (94% of the particles from 19 to 25  $\mu\text{m}$ ), and mean size 37  $\mu\text{m}$  (94% of the particles from 34 to 40  $\mu\text{m}$ ). The blended powders were mechanically alloyed in alumina vials under atmospheric conditions, using a SPEX Mixer 8000 (Sytech Corporation, Houston, TX) mill. Stainless steel ASI 52100 bearing balls from 12 to 16 mm in diameter were used as grinding media. The weight ratio of the powder to balls was kept at 5:1, and duration of milling was varied from 1800 to 2400 s depending on the composition of the powder mixture. In the first stage, the powder contained 20, 30, 50, and 75 vol% of 8  $\mu\text{m}$  SiC, the balance being Al 6061 alloy. The compositions of the MMC are coded using volume percentage and particle size of SiC; for example, Al-75SiC8 denotes a composite with 75 vol% SiC of 8  $\mu\text{m}$  size as the reinforcement. Mechanical alloying was conducted from 1 to 4 wt% additions of stearic acid ( $\text{C}_{18}\text{H}_{36}\text{O}_2$ ) which acted as a process control agent (PCA). The PCA acted as a surfactant and altered the powder characteristics. In the second stage of the investigation, the powder composition was maintained at 50 vol% SiC, and the SiC particle size was varied using the 8, 15, 22, and 37  $\mu\text{m}$  SiC powders. The mechanically alloyed powders were sieved and classified. Composite powder sizes ranging from 44 to 149  $\mu\text{m}$  were used for plasma spraying.

### 2.2 Plasma Spraying Process

Spraying was done in air using an Axial III (Northwest Mettech Corp., Richmond, BC, Canada) plasma torch which operated with an argon plasma gas. All powders were sprayed under the same conditions except for Al-75SiC8, as shown in Table 1. Coating thickness varied from 120 to 220  $\mu\text{m}$ . Some thick coatings ( $\approx 6$  mm) were also produced for the purpose of density measurements. Coatings were sprayed on flat, plain carbon steel coupons, 2.5 cm in diameter and either 1.25 or 2.5 cm long ends of mild steel rods (specimens for ASTM C 633-79 tensile adhesion tests), and 150 to 180  $\mu\text{m}$  thick Al, Ni, plain carbon and stainless steel foils (specimens for peel adhesion test).

### 2.3 Coating Characterization

ASTM C 633 tensile test of adhesion suggests using 1.25 cm long mild-steel rods. Thus, although the longer specimens do not exactly conform to the ASTM standards, they were preferred to avoid the effects of nonuniform stress distribution (Ref 17). The test samples were assembled using a 3M structural epoxy (EC 1386) as an adhesive that has a tensile strength of 120 MPa. A standard Instron machine (Instron Corporation, Canton, MA, model TTC) was used for conducting the tests. Adhesion was also assessed from the peel adhesion test (PAT) which is a modified version of the ASTM D 3167 peel test (Ref 17-21). The PAT samples were made by spraying on the thin Al, Ni, stainless steel, and plain carbon steel foils mounted on copper blocks (Ref 17-21).

The oxygen pickup during spraying was assessed from the height of the aluminum oxide peak, obtained on the surface of the coating from x-ray diffractometry (XRD). The extent of oxidation was also confirmed from the energy dispersive spectroscopy (EDS) analyses of the coatings. Coating density was measured by helium pycnometry after removing the thick coatings ( $\approx 6$  mm<sup>2</sup>) from their substrates.

The abrasive wear test involved samples with  $\approx 1$  cm<sup>2</sup> of the coating, mounted in a hard epoxy resin, Epofix (Struers, Copenhagen, Denmark), abraded under a constant load with 400 grit SiC papers in a Buehler autopolisher Model Ecomet III (Buehler, Ltd., Illinois) in a similar fashion to metallographic polishing. The test is similar to the Abrapol-2 wear test developed by Struers where the abrasive medium is a ceramic slurry (Ref 22). The uniformity of abrasion was maintained by replacing the SiC papers every 180 s. To further maintain the uniformity of wear of the SiC papers, independent of the MMC composition, hard wear resistant chromium oxide coatings were abraded simultaneously along with the composite coatings. Chromium oxide has a wear resistance superior to any of the MMC tested, and this ensured that the rate of wear of the SiC papers was uniform and regular. The material loss due to wear was monitored by measuring the changes in the thickness and weight loss of the specimens.

The erosion wear resistance was assessed by jet nozzle type erosion equipment, a modification of the ASTM G 76-83 test. The ASTM standard suggests that the test be conducted with a grit flow of 0.033 g/s and conducted for 600 s. The erosion experiments were conducted using a commercial grit blaster, Model 3040S (Empire Abrasive Equipment Corporation, PA) with a constant particle velocity of 70 m/s and grit flow rate of 0.92 g/s. The samples were obtained from coupons having coatings of 1 cm<sup>2</sup> surface area. The loss of material due to erosion

**Table 1** Summary of the plasma spraying conditions

| Plasma spraying parameters    | Al-20SiC8 | Al-30SiC8 | Al-75SiC8 |
|-------------------------------|-----------|-----------|-----------|
|                               | Al-50SiC8 |           |           |
| Total gas flow, L/min         | 220       |           | 220       |
| Plasma gas                    | Argon     |           | Argon     |
| Hydrogen content, total gas % | 7.5       |           | 12.5      |
| Current, A                    | 180       |           | 210       |
| Power, kW                     | 66        |           | 79        |
| Powder feed rate, g/s         | 0.5       |           | 0.35      |
| Powder carrier gas            | Argon     |           | Argon     |
| Standoff distance, mm         | 100       |           | 80        |

was calculated from the weight loss of the specimens. Bulk, cast, and extruded samples of Al-20 vol% Al<sub>2</sub>O<sub>3</sub> (having Al<sub>2</sub>O<sub>3</sub> particles of ≈35 μm diameter, in Al 6061 alloy) (Alcan, Montreal, Canada) were used as a reference material for the wear behavior of the coatings developed.

### 3. Results and Discussion

#### 3.1 Powder Preparation

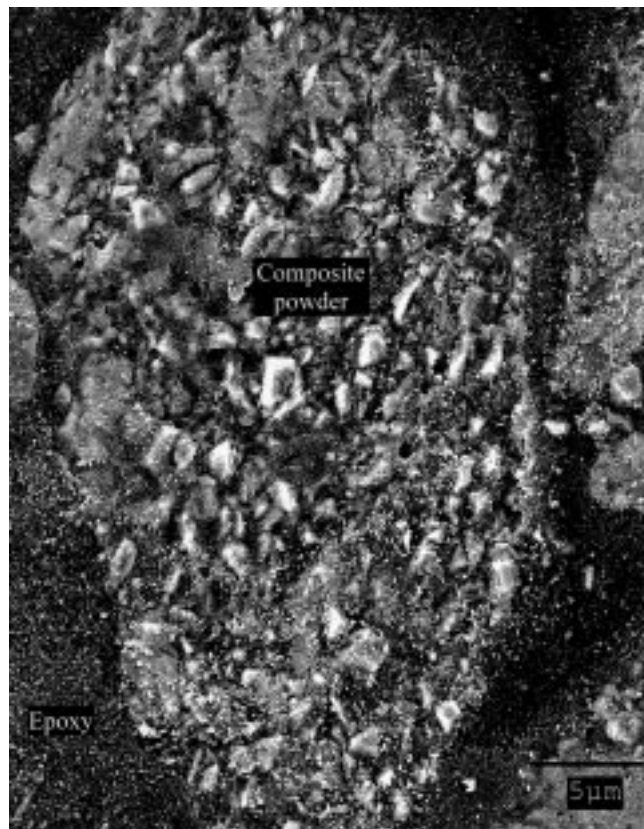
One of the main problems in manufacturing Al-SiC composite powders is agglomeration of the SiC particles in the Al matrix. Mechanical alloying offers one of the better processing routes by which these powders can be produced with minimum segregation. By the use of 3 wt% PCA, the Al particles were fractured and reduced from their initial size of 45 μm to <8 μm. After the initial fracture, the particles agglomerated or cold welded and entrapped the SiC particles. The absorption of the PCA within the agglomerated Al particles allowed an increase in their size with increase in time of milling. The final sprayable composite powders had equiaxial particles ranging from 45 to 200 μm, Fig. 1(a). In comparison, the powder milled without PCA for 1800 s, Fig. 1(b), exhibited a lamellar structure with SiC primarily present on the surface of the MMC particles. Details on the powder production technique and powder morphologies have been presented elsewhere (Ref 24, 25).

Cross-sectional analysis of the powder particles, milled with PCA (Fig. 1a), indicated a uniform distribution of SiC in the aluminum alloy matrix. Comparison of Fig. 1(a) and (b) indicates that for the same duration of milling the distribution of SiC was more homogeneous with PCA. The fracture of Al in the initial stage of milling with PCA allowed a more homogeneous distribution of SiC within the Al matrix. The absence of PCA limited the fracture of the Al particles, and the SiC reinforcements were concentrated near the surface of the MMC powder.

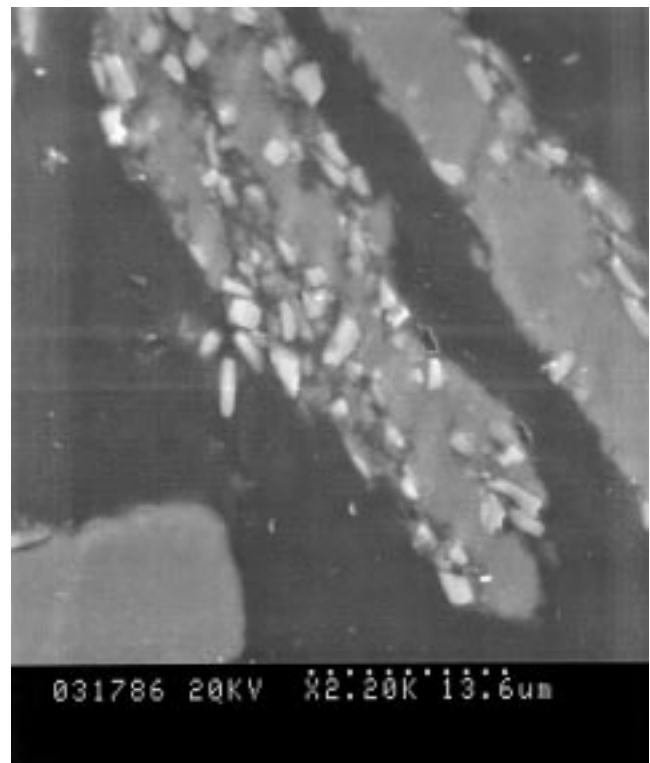
#### 3.2 Coating Characteristics

The coatings show a dense and clean microstructure with little smearing and some isolated pores, Fig. 2(a) and (b). The isolated pores (darkened areas in the microstructure) may have been a result of SiC pullouts during polishing. No unmelted particles of Al 6061 alloy were encountered in the microstructure. Some oxide contamination was observed in the coatings and was confirmed by the XRD results of the same which showed traces of Al<sub>2</sub>O<sub>3</sub> formation (Fig. 3). The XRD analyses did not indicate any possible reactions between Al and SiC particles, in particular the formation of Al<sub>4</sub>C<sub>3</sub>. The observed densities approach 98% of the theoretical values indicating very little porosity within the coatings.

The SiC in the coatings has a distribution, composition, and morphology similar to that in the powders sprayed. The presence of SiC was confirmed by x-ray analyses of the coatings



(a)



(b)

**Fig. 1** (a) Cross section of an Al-50SiC8 powder milled for 1800 s with process control agent (PCA) as an additive. (Art has been reduced to 43% of its original size for printing.) (b) Cross section of an Al-50SiC8 powder milled for 1800 s without PCA. (Art has been reduced to 42% of its original size for printing.)



which showed a distinct SiC peak in addition to the Al peak (Fig. 3). The SiC was distributed as individual particles in the matrix as shown in Fig. 2(a) and (b), with limited clustering. The distribution of SiC was studied by using back scattered x-ray mapping of Si. Figure 2(c) shows the Si mapping of the Al-50SiC8 coating (Fig. 2b) indicating some clustering of SiC (areas devoid of white spots). The uniformity of SiC distribution in the coatings was assessed quantitatively by measuring the interparticle distance ( $\lambda$ ) between the SiC particles. The interparticle distance was measured by the random intercept technique (Ref 14). The typical distribution histograms of the interparticle distance (ID) for some of the composites is shown in Fig. 4.

The change in average ID with SiC content and size are summarized in Fig. 5 and 6, respectively. As expected, with the increase in the SiC content the ID decreased. The ID increased with the increase in the size of the second phase (Fig. 6). The variation of the interparticle distance, indicated by the standard deviation (SD) of the ID, decreased with increase in the content of SiC in the matrix. The variations are also shown on the respective plots in Fig. 5 and 6. The Al-20SiC8 showed the highest variation, and the Al-75SiC8 had the least variation among the 4 coatings with the 8  $\mu\text{m}$  particle size reinforcements. Similarly, the variation in ID values was found to decrease with increase in the SiC particle sizes. Thus, the homogeneity of the coatings improved with increase in the SiC particle size and with the increase in the volume percentage of SiC in the composites. Similar results were reported by Stone and Tsakirooulos (Ref 14).

### 3.2.1 Adhesion Tests

Tensile adhesion tests (TAT) conducted according to the ASTM standard C 633-79 test proved to be inconclusive because very few failures were limited to the coating/substrate interface. Results obtained from the TAT are summarized in Table 2. Most of the failures occurred at loads from 68 to 75 MPa and

were located between the epoxy-coating or the epoxy-substrate interfaces. Due to the inconclusive nature of the results obtained with 8  $\mu\text{m}$  sized SiC composites, the TAT was not conducted for compositions other than those mentioned in Table 2.

The peel adhesive test (PAT) results for the different powder compositions on different substrates are summarized in Table 3. A typical peel strength curve of the composite powder is shown in Fig. 7. The peel force curve in Fig. 7 shows significant variations. The variations resulting from the test process itself have been estimated to be  $\approx 10\%$  of the average peel strength (Ref 19). Thus, many of the larger variations in peel strength can be attributed to surface defects on the substrate or macrostructure of the coating in that localized zone, for example, porosity and microcracks. The values of peel strength in Table 3 include the plastic work done on foil during peeling and the friction between the foil and the mandrel (Ref 17, 21). The peel strength values in

**Table 2 Summary of the ASTM C 633 pull adhesion test results (MPa)**

| Substrate material | Al-20 SiC8 | Al-30 SiC8 | Al-50 SiC8 | Al-75 SiC8 |
|--------------------|------------|------------|------------|------------|
| Aluminum           | 75         | 72         | 76         | 68         |
| Mild steel         | 68         | 72         | 69         | 70         |

**Table 3 Summary of the peel test strength (N/m)**

| Foil material   | Foil thickness, ( $\mu\text{m}$ ) | Foil thickness, ( $\mu\text{m}$ ) |             |             |              |              |              |
|-----------------|-----------------------------------|-----------------------------------|-------------|-------------|--------------|--------------|--------------|
|                 |                                   | Al-30 SiC 8                       | Al-50 SiC 8 | Al-75 SiC 8 | Al-50 SiC 15 | Al-50 SiC 22 | Al-50 SiC 37 |
| Ni              | 178                               | 2460                              | 1760        | 1415        | 1820         | 1925         | 2140         |
| Steel           | 178                               | 950                               | 780         | 595         | ND           | ND           | ND           |
| Stainless Steel | 102                               | 530                               | 510         | 510         | ND           | ND           | ND           |
| Al              | 76                                | ND                                | >2880       | ND          | ND           | ND           | ND           |
|                 | 152                               | ND                                | 3180        | ND          | 3330         | 4060         | 4690         |

ND indicates not determined.

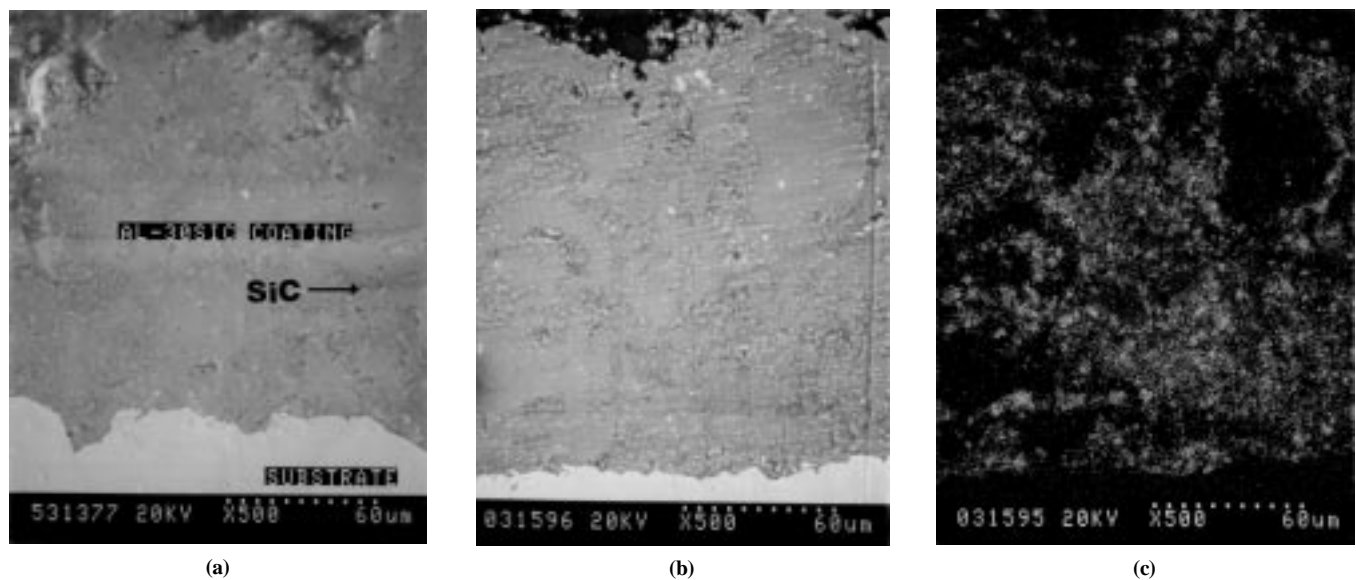


**Fig. 2** (a) Cross section of Al-30SiC8 coating. (b) Cross section of Al-50SiC8 coating. (c) Si mapping of the Al-50SiC8 coating in (b)

Fig. 8 and 9 were obtained after eliminating the plastic work and the work done due to friction.

The adhesion strength of the coating was highest when Al substrates were used. Nickel showed the next highest average peel strength for a given composition of the powder, while stain-

less steel (SS) showed the lowest adhesion strength. Sexsmith et al. (Ref 17-20) obtained a correlation between the yield stress of the substrate and the peel strength obtained for a given coating material. A low yield stress allows an easier accommodation of the residual stress built up at the interface during spraying and

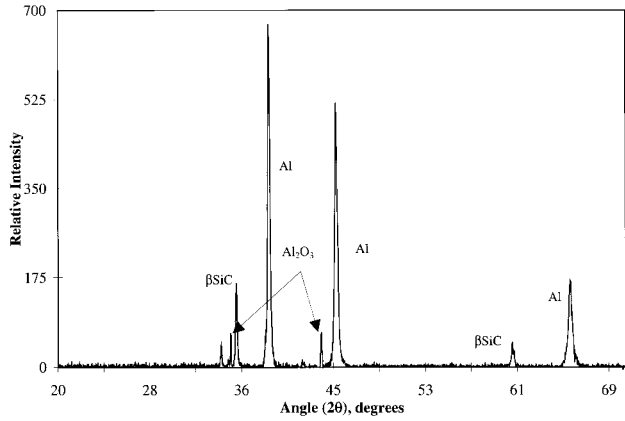


**Fig. 3** X-ray diffraction (XRD) pattern of Al-30SiC8 coatings showing Al<sub>2</sub>O<sub>3</sub> contamination

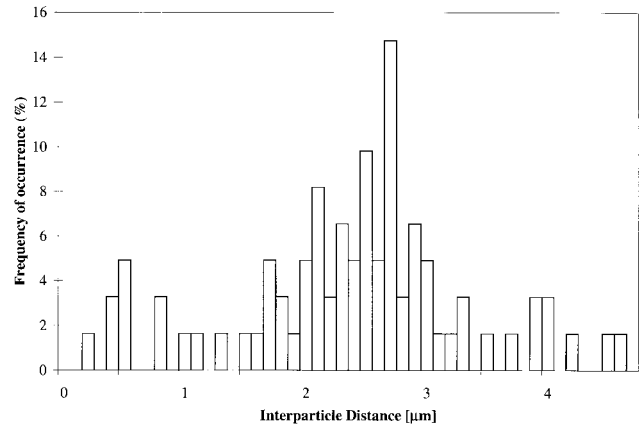


**Fig. 4** Distribution of the interparticle distance of Al-50SiC8 coatings

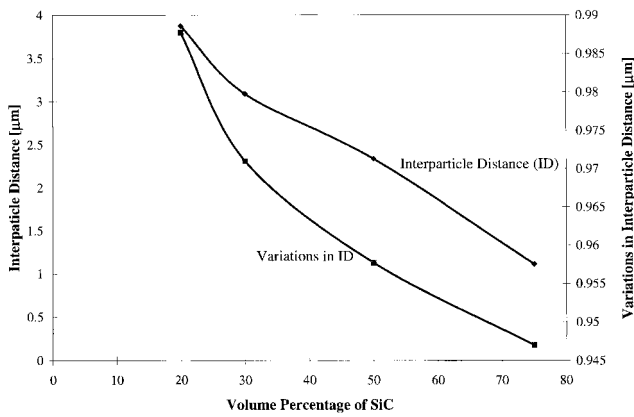


**Fig. 5** Change in average interparticle distance with SiC content in the Al-SiC composite

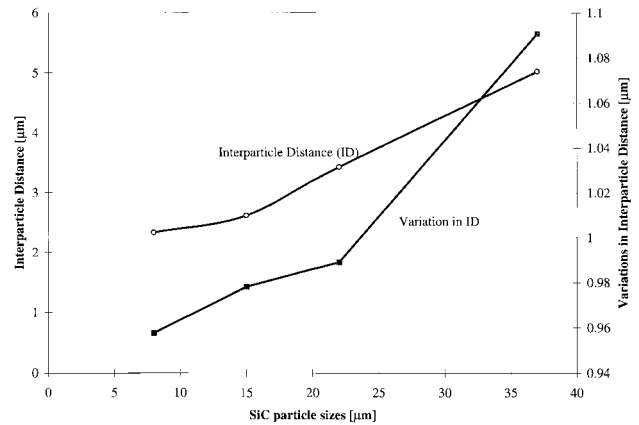


**Fig. 6** Change in average interparticle distance with SiC particle sizes in Al-50vol%SiC composite

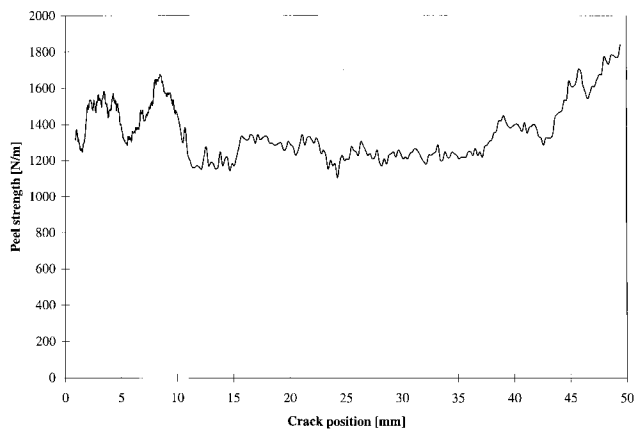


**Fig. 7** Peel strength of an Al-50SiC37 coating deposited on nickel

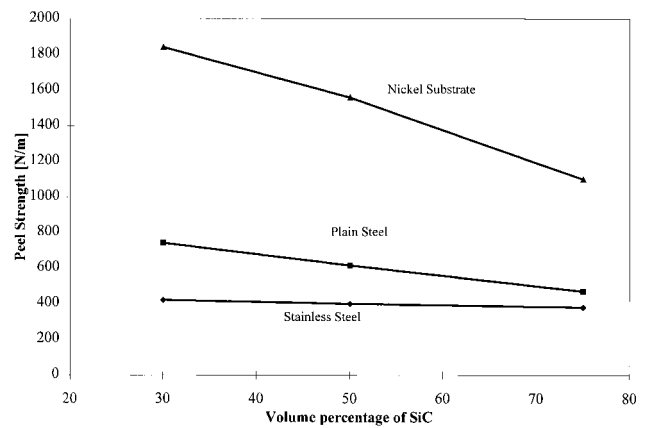


**Fig. 8** Variation of the average peel strength with SiC content for different substrates

thereby improving adhesion strength. Thus, the low yield stress of Ni, compared to that of steel is one probable reason for the high peel strength.

There are two possible arguments for the high adhesion strength shown by Al substrates. Al has a lower yield stress than Ni and thus can accommodate higher residual stresses at the interface. Also, as shown in Fig. 10, there is fusion at the surface of the Al foil substrates on contact with the sprayed coatings. The low melting point of Al (667 °C) allows incipient fusion of

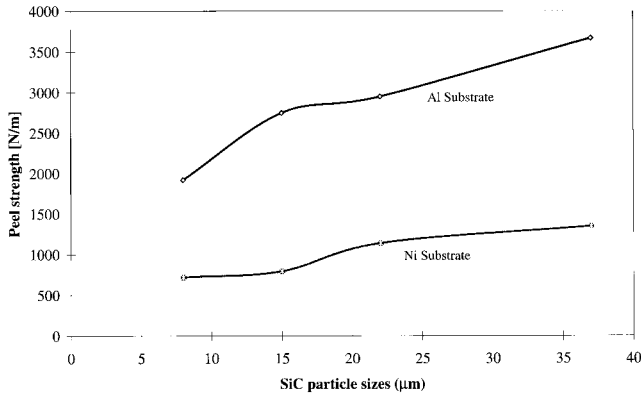
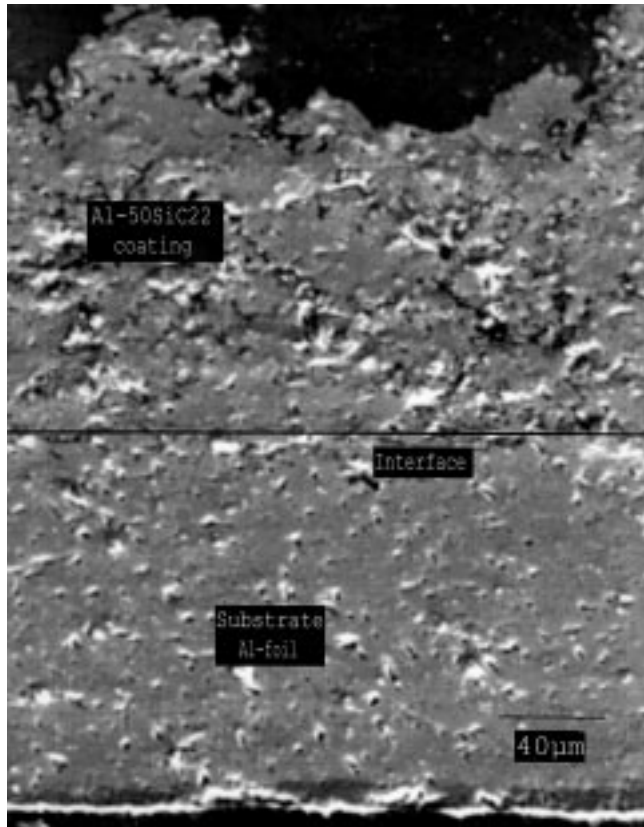
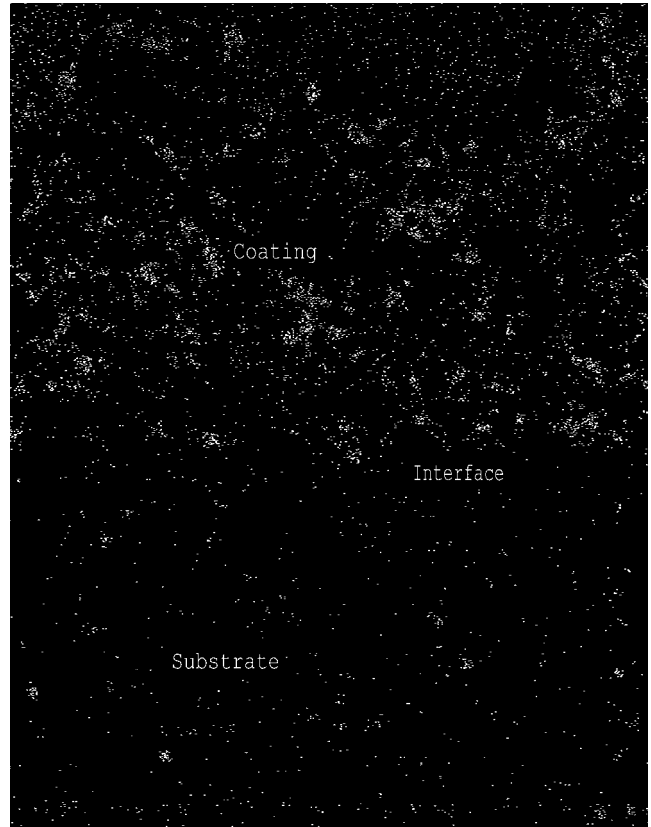


**Fig. 9** Variation of the peel strength with the SiC particle size in the Al-SiC composites



(a)



(b)

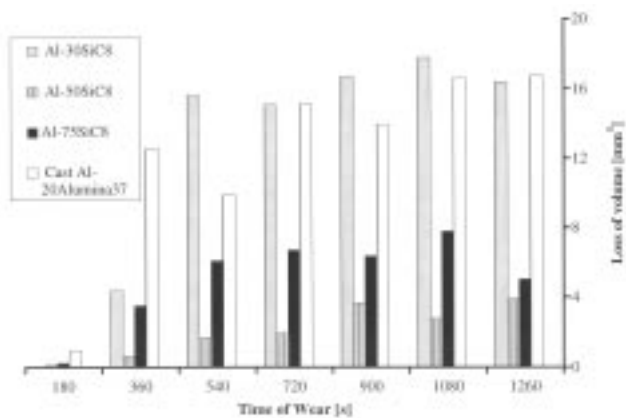
**Fig. 10** (a) Al-50SiC22 coating on an Al foil showing absence of a regular interface. (b) Si map of (a) showing the distribution of the SiC. (Art has been reduced to 43% of its original size for printing.)

the substrate, and this allows the formation of a continuous medium with the molten Al, thereby eliminating a regular interface.

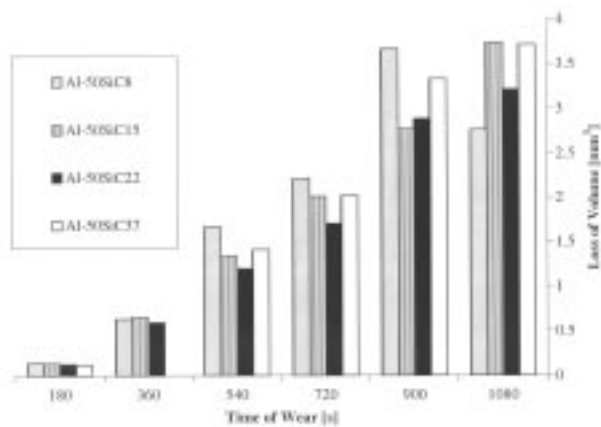
The change in average peel strength with SiC content and SiC particle size is shown in Fig. 8 and 9, respectively. The variation in peel strength with SiC content and size was most noticeable with Al and Ni substrates. The peel strength decreased with increase in SiC content and increased with the increase in SiC particle sizes for all the different substrates used in this investigation. This can be correlated to the changes in ID, with increasing concentration and decreasing size of the SiC reinforcements, as shown in Fig. 5 and 6, respectively. The decrease in the ID reduces the area fraction of metal in contact with the substrate at the interface. Since metallic coatings have a higher adhesion strength (Ref 18-20), the decrease in metal content at the interface reduces the peel strength of the composite. Moreover, since the Al in the MMC only melts during spraying, there is only mechanical bonding between the SiC particles and the substrates.

### 3.2.2 Wear Tests

The results of the abrasive wear tests under 35 N, using SiC abrasive papers, are shown in Fig. 11(a) and (b): These figures illustrate the changes in abrasive wear rate with SiC content and SiC particle sizes, respectively. The wear resistance of all the coatings was superior or similar to the Al-20 vol%, Al<sub>2</sub>O<sub>3</sub> cast, and extruded reference material. The wear resistance of the composites showed an optimum at 50 vol% SiC content; see Fig.



(a)



(b)

**Fig. 11** Change in abrasive wear resistance with SiC content under a load of 35 N for the Al-SiC composites containing (a) 8  $\mu\text{m}$  large SiC and (b) 50 vol% SiC

11(a). Further increase in the SiC content decreased the wear resistance. In the second stage of the investigation, the abrasive wear resistance of Al-50SiC22 was higher than the other coatings of the same composition. By a comparison of the wear behavior under different loads, experimental errors were able to be estimated. For example, in the instances that wear volume decreased with increase in wear time can be attributed to the experimental errors.

Hwang and Chung (Ref 22) suggested three possible mechanisms for the SiC to break loose from the surface: brittle fracture, pull out from the matrix, or subsurface ductile fracture in the Al alloy matrix and the SiC particles are carried away when the latter detaches. The load of 35 N was not high enough to cause brittle fracture of the SiC particles. Besides, the Al 6061 alloys show a good interface strength which makes them one of the most popular matrix alloys for particle reinforced Al composites. Therefore, it is not likely that the SiC pulls out. The investigation of the abraded surfaces under SEM (Fig. 12) indicates the subsurface fracture to be the dominant mechanism, which has been confirmed elsewhere (Ref 23). Thus, with an increase in SiC particle size, the propagation of the subsurface fracture is limited, and this improves the wear resistance. Similarly, the increase in the volume fraction of the reinforcements

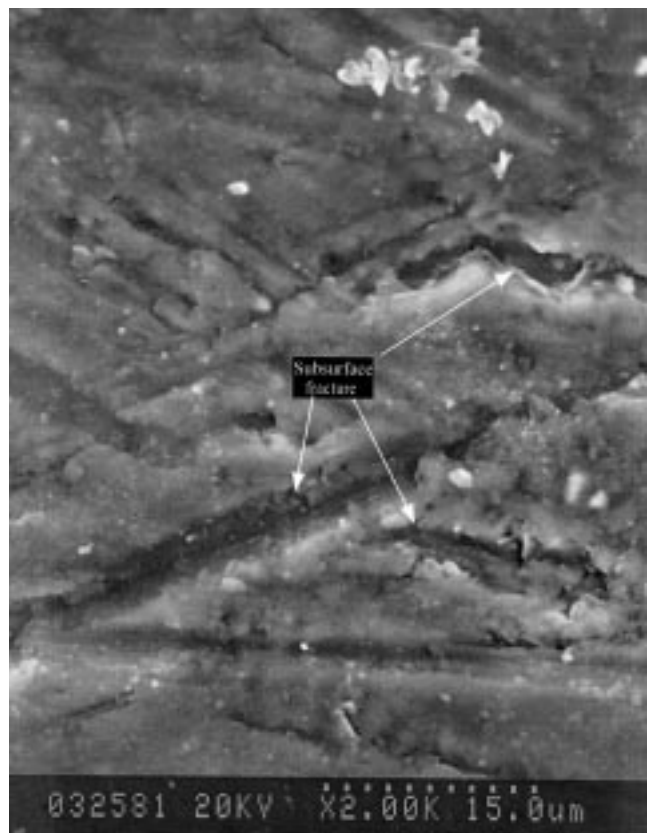


**Fig. 12** Abraded surface of Al-50SiC15 coating showing plastic deformation of the Al matrix. (Art has been reduced to 43% of its original size for printing.)

results in increased deviation of the subsurface crack and improved wear resistance. The lower wear resistance in the Al-75SiC8 composites is due to the reduced matrix content resulting in pullouts.

The results of the erosive wear tests are summarized in Fig. 13(a) and (b) showing the variation in erosive wear resistance with SiC content and particle size, respectively. The erosive wear resistance improved with increase in SiC content. Al-75SiC8 showed the highest erosive wear resistance. The increase in SiC particle size decreased the erosive wear resistance. Al-50SiC15 coatings showed a higher erosive wear resistance among the four coatings of that composition (Fig. 13).

Deformation and removal of the ductile Al is believed to be the dominant erosive wear mechanism. The typical wear surface of the Al-50SiC15 coating is shown in Fig. 14. The extent of wear depends on the size and depth of the indentation left from the impact of the individual striking particles, and the indentation size depends on the interlamellar spacing. The increase in SiC particle size increases the interparticle distance, and this exposes a greater area of the matrix Al to the erosive medium. Since removal of Al is the dominant mechanism, the erosive wear resistance decreases with increasing SiC particle size. Although Al-50SiC8 had the least interparticle distance, it did not show the highest wear resistance among the coatings of same composition. This could be because of the microstructural inhomogeneity of the Al-50SiC8 coatings compared to that of Al-50SiC15 coatings. The inhomogeneity produces clustered areas

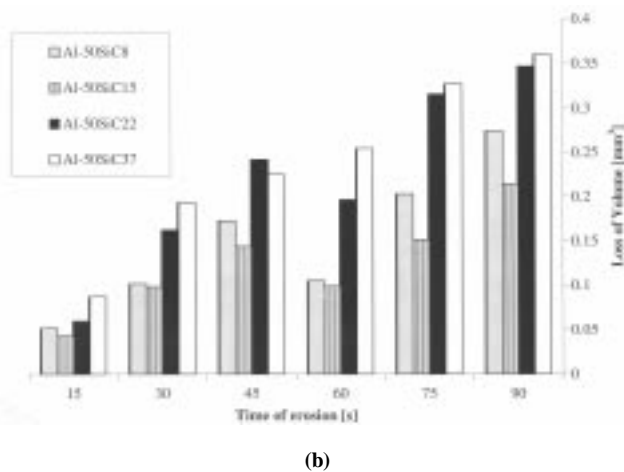
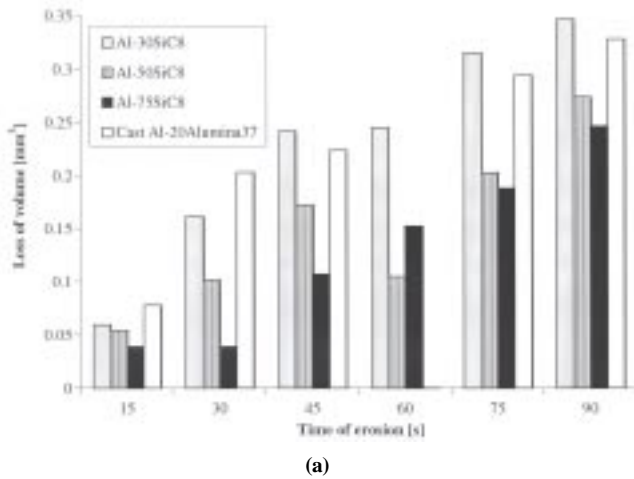


**Fig. 13** (a) Variation of erosive wear resistance with SiC content in the Al-SiC composites containing 8  $\mu\text{m}$  large SiC. (Data for the wear of the reference cast composite material was not available for  $t = 60$  s.) and (b) change in erosion wear resistance with SiC particle sizes for the Al-SiC composites containing 50 vol% SiC

in the microstructure (Fig. 2b), with high concentration of SiC and having other areas devoid of any reinforcement. Thus, the Al-50SiC15 coatings had the highest erosive wear resistance among the coatings of Al-50vol%SiC compositions.

## 4. Conclusions

An attempt was made to develop a method to improve the surface properties of Al by plasma spraying MMC coatings with SiC as reinforcements. The present work consisted of developing homogeneous, plasma sprayable Al-SiC composite powders, plasma spraying of these powders, and assessing the properties of the plasma sprayed coatings. These plasma sprayed coatings include adhesion strength, density, abrasion, and erosion resistance. The process of mechanical alloying using a SPEX mixer mill was used to produce MMC powders with a uniform distribution of SiC in the Al matrix. The use of PCA improved the efficiency of mechanical alloying. The following

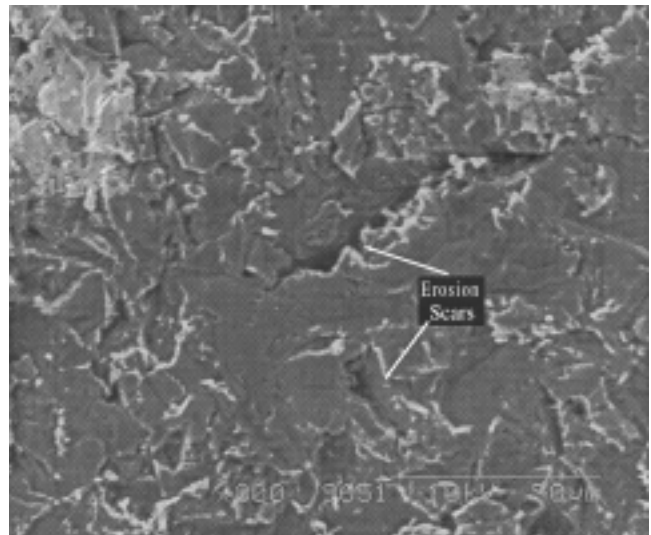


**Fig. 14** Erosion surface of Al-50SiC15 coating showing erosion scars and plastic deformation of the matrix. (Art has been reduced to 74% of its original size for printing.)

conclusions can be drawn based on the results obtained in the present investigation.

- The plasma sprayed Al-SiC composite powders produced dense ( $\approx 98\%$  of theoretical value) homogeneous coatings.
- The adhesion strength of the coatings increased with increase in SiC particle size and was proportional to the content of Al in the composite. Al substrates showed the highest adhesion strength for any given composition of the coating, due to formation of a metallurgical bond between the coating and the substrate.
- The abrasive wear resistance of the coatings was superior to the commercially available Al-20vol%Al<sub>2</sub>O<sub>3</sub> composites. The increase in SiC content from 30 to 50 vol% of the plasma sprayed MMC increased the wear resistance. However, the wear resistance decreased for the 75 vol% SiC coatings. Among the four SiC particle sizes with 50 vol% of the reinforcements used in the present investigation, Al-50SiC22 containing 22  $\mu\text{m}$  large SiC particles showed the best abrasion resistance.
- The erosion resistance of the Al-SiC coatings was directly proportional to the SiC content. Consequently, Al-75SiC8 showed the best erosion wear resistance among the coatings with the same size reinforcement particles. The erosion wear resistance decreased with increase in the SiC particle size.

The present investigation indicates that Al-SiC coatings can improve the surface wear resistance of structural Al components without producing any significant change in the ductility of the component. The wear resistance of the coating was comparable to or better than the commercially available cast Al-20Al<sub>2</sub>O<sub>3</sub> composites, thereby providing an alternative to the costly manufacture of structural MMC components. Alternatively, the composites can also be used as a material for surface repair of worn structural MMC.



## Acknowledgments

The authors wish to acknowledge technical assistance provided by Northwest Mettech, Vancouver, Canada for plasma spraying the powders. A special thanks is extended to Edith Breslauer for assisting in calibrating and performing the peel tests. Additionally, the authors wish to acknowledge SCBC and NSERC for funding the project and NRC for access to wear testing equipment.

## References

1. T. Imura, T. Suenaga, T. Hayashi, and H. Ushio, "Application of Metal Matrix Composites for Connecting Rods and Cylinder Blocks," SAE Technical Paper 890557, 1989, p 1-8
2. G.S. Cole and F. Bin, Scuffing Resistance of Al-Based MMCs as Bores in Aluminum Engine Blocks, *Proceedings of the ASM 1993 Materials Congress*, ASM International, 1993, p 13-20
3. J.F. Garneau, R. Angers, M.R. Krishnadev, and L. Collins, "Fabrication and Characterization of SiC/6061 Composites," 32nd. Annual Conf. of Metallurgists of Canadian Institute of Metallurgy, 1993, P 27-36
4. M. Sternitzke, M. Knetchel, M. Hoffman, E. Broszeit, and J. Rodel, Wear Behavior of Alumina/Aluminum Composites with Interpenetrating Networks, *J. American Ceramic Society*, Vol 79 (No. 1), 1996, p 121-128
5. P.V. Ananthapadmanabhan, K. Sreekumar, P.V. Ravindran, N. Venkatramani, and S.C. Mishra, *Characterisation of Plasma Spheroidised Nickel—Aluminum Powder, Thermal Spraying—Current Status and Future Trends*, A. Ohmori, Ed., High Temperature Society of Japan, Osaka, 1995, p 1127-1131
6. M.I. Boulos, P. Fauchais, and E. Pfender, "Advances in Therm. Spraying," (short course,) ASM International, June 1993, Anaheim, California
7. T.H. Stenberg, K.J. Niemi, P.M.J. Vuoristo, J.E. Vuorinen, T.A. Mantyla, and T.J. Tianen, Effect of Powder Manufacturing Method, Particle Size and Binder Content on the Properties of TiC-Ni Composite Coatings, *Thermal Spraying—Current Status and Future Trends*, A. Ohmori, Ed., High Temperature Society of Japan, Osaka, 1995, p 1145-1150
8. J.S. Benjamin and R. Schelleng, Dispersion Strengthened Aluminum-4% Magnesium Alloy Made by Mechanical Alloying, *Metall. Trans. A*, Vol 12, 1981, p 1827-1832
9. L. Lu, M.O. Lai, and S. Zhang, Preparation of Al-Based Composite using Mechanical Alloying, *Key Engineering Mater.*, Vol 37, May 1995, p 212-220
10. J. Kaneko, M. Sugamata, and R. Horiuchi, *Mechanical Alloying of Aluminum with Ceramic Particles*, Eighth. Int. Light Metals Congress, Leoben, Vienna, 1987, p 776-780
11. A. Bhaduri, A.N. Tiwari, V. Gopinathan, and P. Ramakrishnan, Studies on Mechanically Alloyed 7010 Aluminum Alloy-SiC<sub>p</sub> Composites, *Mater. Sci. Forum*, Vol 88-90, 1992, p 205-212
12. P.S. Gilman and J.S. Benjamin, Mechanical Alloying, *Ann. Rev. Mater. Sci.*, Vol 13, 1983, p 279-300
13. G. Mahanty, A.N. Tiwari, V. Gopinathan, and P. Ramakrishnan, Studies on Mechanically Alloyed 7010 Aluminum Alloy - SiC Composites, *Key Eng. Mater.*, Vol 29-31, 1989, p 747-754
14. I.C. Stone and P. Tsakiroopoulos, Characterization of Spatial Distribution of Reinforcement in Powder Metallurgy Route Al/SiC<sub>p</sub> Metal Matrix Composites; Part 1—Techniques Based on Microstructure, *Mater. Sci. and Technol.*, Vol 11, March 1995, p 213-221
15. A. Ilyuschenko, P. Vityaz, V. Okovity, A. Verstak, E. Lugscheider, and P. Remer, *Investigation of APS and CDS Process of Formation Al-Carbide and AlSi-Carbide Coatings*, Advances in Thermal Spray Science & Technology, C.C. Berndt and S. Sampath, Ed., ASM International, 1995, p 317-320
16. K.A. Khor, Y. Murakoshi, and T. Sano, "Plasma Spraying of Al-Li Based Metal Matrix Composites, *Thermal Spraying—Current Status and Future Trends*," A. Ohmori, Ed., High Temperature Society of Japan, Osaka, 1995, p 1133-1137
17. M. Sexsmith, T. Troczynski, and E. Breslauer, Plastic Work in the Peeling of Work Hardening Foils, *J. Adhesion Sci. Technol.*, Vol 11 (No. 2), 1997, p 141-154
18. M. Sexsmith and T. Troczynski, "Development of Peel Adhesion Test for Thermal Sprayed Coatings," *Thermal Spraying—Current Status and Future Trends*, A. Ohmori, Ed., High Temperature Society of Japan, Osaka, 1995, p 897-902
19. M. Sexsmith and T. Troczynski, Peel Adhesion of Thermal Sprayed Coatings, *J. Therm. Spray Technol.*, Vol 5 (No. 2), 1996, p 196-206
20. M. Sexsmith and T. Troczynski, Variation in Coating Properties Across a Spray Pattern, *Thermal Spray Industrial Applications*, C.C. Berndt and S. Sampath, Ed., ASM International, 1994, p 751-757
21. E. Breslauer and T. Troczynski, Experimental Determination of Peel Adhesion Strength for Metallic Foils, *J. Adhesion Sci. Technol.*, (submitted for publication)
22. S. Chung and B.H. Hwang, A Microstructural Study of the Wear Behavior of the SiC<sub>p</sub>/Al Composites, *Tribology International*, Vol 27 (No. 5), 1994, p 307-314
23. K. Muller and E. Fundal, Description of the Microwear Test and Application Studies, *Proc. of Nordic Conference on Tribology*, Hirtshals, Denmark, 1990, p 499-515
24. K. Ghosh, T. Troczynski, and A.C.D. Chaklader, "Al-SiC Metal Matrix Composite Coatings by Plasma Spraying," *Thermal Spray: Practical Solutions for Engineering Problems*, C.C. Berndt, Ed., ASM International, 1996, p 339-347
25. K. Ghosh, T. Troczynski, and A.C.D. Chaklader, Processing of Composite Al-SiC Powders for Plasma Spraying, *Powder Metall. Int.*, (submitted for publication)